Published in final edited form as:
Nat Cell Biol. 2009 February ; 11(2): 143–153. doi:10.1038/ncb1819.

SRF and myocardin regulate LRP-mediated amyloid-β clearance in brain vascular cells

Robert D. Bell[1], **Rashid Deane**[1], **Nienwen Chow**[2], **Xiaochun Long**[3], **Abhay Sagare**[1], **Itender Singh**[1], **Jeffrey W. Streb**[3], **Huang Guo**[1,2], **Anna Rubio**[2], **William Van Nostrand**[4], **Joseph M. Miano**[3,5], and **Berislav V. Zlokovic**[1,5,6]

1*Center for Neurodegenerative and Vascular Brain Disorders, Arthur Kornberg Medical Research Building, University of Rochester School of Medicine & Dentistry, 601 Elmwood Avenue, Rochester, New York 14642, USA.*

2*Socratech Research Laboratories, University of Rochester School of Medicine & Dentistry, 601 Elmwood Avenue, Rochester, New York 14642, USA.*

3*Aab Cardiovascular Research Institute, University of Rochester School of Medicine & Dentistry, 601 Elmwood Avenue, Rochester, New York 14642, USA.*

4*Department of Medicine, Stony Brook University, Stony Brook, New York 11794, USA.*

Abstract

Amyloid β-peptide (Aβ) deposition in cerebral vessels contributes to cerebral amyloid angiopathy (CAA) in Alzheimer's disease (AD). Here, we report that in AD patients and two mouse models of AD, overexpression of serum response factor (SRF) and myocardin (MYOCD) in cerebral vascular smooth muscle cells (VSMCs) generates an Aβ non-clearing VSMC phenotype through transactivation of sterol regulatory element binding protein-2, which downregulates low density lipoprotein receptor-related protein-1, a key Aβ clearance receptor. Hypoxia stimulated SRF/MYOCD expression in human cerebral VSMCs and in animal models of AD. We suggest that SRF and MYOCD function as a transcriptional switch, controlling Aβ cerebrovascular clearance and progression of AD.

Dementia in Alzheimer's disease (AD) is associated with neurovascular dysfunction[1,2] and accumulation of neurotoxic amyloid β-peptide (Aβ) in the wall of cerebral blood vessels and in the brain[1–4]. Aβ deposition in VSMCs of small cerebral arteries contributes to cerebral amyloid angiopathy (CAA)[1,2,5], the prevalence of which is greater than 80% in AD individuals and 10–40% in the elderly population without AD[5,6]. CAA is associated with cognitive impairment[5]. Microbleeds in the brain occur in 80% of CAA cases and in 30% of AD patients with CAA[7], whereas lobar cerebral haemorrhage occurs in 7–18% of AD cases[5].

Recent work has suggested that Aβ accumulates in the wall of cerebral vessels and in brains of AD individuals because of its impaired clearance from the brain and/or imbalances between its production and clearance[2,3,8–10]. In mouse models of familial AD expressing the Swedish

6Correspondence should be addressed to B.V.Z. (e-mail: berislav_zlokovic@urmc.rochester.edu).
5J.M.M. and B.V.Z. were co-senior authors.

Note: Supplementary Information is available on the Nature Cell Biology website.

COMPETING FINANCIAL INTERESTS
The authors declare no competing financial interests.

Published online at http://www.nature.com/naturecellbiology/
Reprints and permissions information is available online at http://npg.nature.com/reprintsandpermissions/

mutation in the Aβ-precursor protein (*APPsw*$^{\pm}$), or harbouring the Dutch and Iowa vasculotropic *APP* mutations, the dense plaques may develop initially on blood vessels or as classical CAA[11–13] because of inefficient Aβ clearance across the blood-brain barrier (BBB) and/or perivascular Virchow-Robin arterial spaces, respectively[1–3]. The low-density lipoprotein receptor-related protein 1 (LRP) is a major Aβ clearance receptor at the BBB[12, 14–17] and in cerebral VSMCs[18].

The molecular basis of CAA is unclear. Recently, we reported that serum response factor (SRF)[19] and myocardin (MYOCD)[20,21], two interacting transcription factors that control VSMC differentiation, are overexpressed in AD and produce a hypercontractile VSMC phenotype in small cerebral arteries through directed expression of SRF–MYOCD-regulated contractile genes[22]. Here, we show that SRF and MYOCD control Aβ clearance from cerebral VSMCs in AD, as well as the degree of CAA and focal Aβ brain accumulations in animal models of CAA and AD. We demonstrate that SRF and MYOCD overexpression in cerebral VSMCs in AD and in mice *in vivo* generates an Aβ non-clearing VSMC phenotype through LRP downregulation, which is mediated by the SRF–MYOCD-directed transactivation of the sterol regulatory element binding protein-2 (SREBP2)[23], an LRP transcriptional repressor[24,25].

RESULTS

SRF and MYOCD block Aβ clearance in cerebral VSMCs

SRF and MYOCD are overexpressed in cerebral VSMCs in AD patients with CAA[22]. Western blot analysis of small cerebral leptomeningeal arterial blood vessel homogenates from AD individuals with CAA showed elevated levels of SRF and MYOCD, Aβ accumulation and significantly lower levels of LRP, compared with age-matched, non-demented controls without CAA (Supplementary Information, Fig. S1a–c). As Aβ does not influence SRF and MYOCD expression in VSMCs[22], we hypothesized that if the association between Aβ accumulation in the vessel wall and SRF/MYOCD overexpression in cerebral VSMCs in AD was not due to chance, then overexpression of SRF and MYOCD may influence clearance of Aβ from VSMCs. To test this hypothesis, we compared clearance of Cy3-labelled Aβ aggregates by cultured cerebral VSMCs isolated from small intracerebral and leptomeningeal arteries from late-stage AD individuals with CAA and age-matched controls without CAA, using a model similar to that reported for Aβ clearance by cultured astrocytes[26]. In all studies, VSMCs were early first-passage cells. (see Methods and Supplementary Information, Table S1 for clinical and neuropathological characteristics of AD individuals and controls). Compared with control VSMCs, AD VSMC showed a decrease in Aβ clearance of more than 70% (Fig. 1a, e), and expressed consistently higher levels of SRF and MYOCD (Fig. 1d), as reported previously[22], and significantly lower levels of LRP (Fig. 2b). Thus, changes in SRF, MYOCD and LRP expression in cultured cerebral VSMCs from AD cases, compared with controls, correlated well with changes in their respective expression levels in cerebral pial arteries in brains *in situ* (Supplementary Information, Fig. S1a–c).

To address whether reducing SRF expression improves Aβ clearance in cerebral VSMCs in AD, we silenced SRF by adenoviral-mediated transduction of AD VSMCs with a short hairpin RNA against *SRF* (Ad.sh*SRF;* moi 100). This decreased levels of both SRF and MYOCD to approximately their respective levels found in controls (Fig. 1d). In some experiments, lower-molecular-weight SRF species, corresponding to spliced or cleaved SRF (data not shown) were also present, as reported for human VSMCs[22]. Reduced MYOCD levels are consistent with earlier reports showing that silencing *SRF* in VSMCs results in downregulation of MYOCD[22] and that its expression is sharply reduced in *Srf*-null mice[27–29]. Ad.sh*SRF*, but not control sh*GFP* (Fig. 1d), substantially improved Aβ clearance by AD VSMCs (Fig. 1b, e). These data indicate that SRF overexpression in cerebral VSMCs from AD individuals decreases Aβ clearance.

Next, we transduced control human cerebral VSMCs with Ad.*MYOCD* to determine whether overexpression of MYOCD would generate an AD-like, Aβ non-clearing phenotype. *MYOCD* gene transfer upregulated both MYOCD and SRF (Fig. 1d) and decreased Aβ clearance by 65% (Fig. 1c, e). MYOCD upregulated SRF, as reported previously[22], by augmenting *SRF* promoter activity, most likely in a CArG-dependent manner (data not shown). Findings from 8 AD cases and 7 controls are summarized in Fig. 1e. Clearance of Cy3-labelled Aβ40 was also reduced in AD VSMCs, compared with controls (Fig. 1f). *MYOCD*, but not *GFP*, gene transfer to control VSMCs decreased Aβ40 clearance by more than 100% (Fig. 1f). These findings demonstrate that MYOCD and SRF overexpression in normal human cerebral VSMC phenocopies the Aβ non-clearing AD-like phenotype.

SRF and MYOCD downregulate LRP in cerebral VSMC

As LRP, a key Aβ clearance receptor, is downregulated in AD cerebral vessels *in situ*[12,14,30] (Supplementary Information, Fig. S1a, c), we next studied whether alterations in SRF and MYOCD expression in cerebral VSMCs affect LRP- mediated Aβ clearance. First, we showed that, in contrast to wild-type embryonic mouse fibroblasts ($Lrp^{+/+}$), $Lrp^{-/-}$ fibroblasts cannot clear Aβ aggregates, confirming the requirement of LRP for Aβ clearance (Supplementary Information, Fig. S1d). Aβ clearance in human cerebral VSMCs was inhibited by the receptor associated protein (RAP), which inhibits binding of Aβ and other LRP ligands to LRP[12], by LRP silencing with Ad.sh*LRP* or by an LRP-specific blocking antibody (Supplementary Information, Fig. S1e). Transduction of VSMCs with control Ad.sh*GFP* did not alter LRP expression. In VSMCs transduced with Ad.sh*LRP*, the addition of RAP abolished Aβ clearance (Supplementary Information, Fig. S1e).

Figure 2a (left panel) illustrates internalization of Aβ aggregates by control VSMCs and their colocalization with lysosomes. As expected, RAP (data not shown) or an LRP-specific antibody inhibited Aβ internalization and its lysosomal association (Fig. 2a, right), confirming that LRP is essential for both steps. LRP levels were significantly reduced in cultured AD VSMCs, compared with controls($P < 0.05$, Fig. 2b), corroborating *in vivo* findings[12,30,31] (Supplementary Information, Fig. S1a, c). Ad.sh*SRF*, but not Ad.sh*GFP*, normalized LRP expression in AD VSMCs (Fig. 2b) and significantly increased Aβ clearance (Fig. 1b, e). Increased LRP protein level was accompanied by increased *LRP* mRNA levels of more than 4-fold (Fig. 2c). In contrast, *MYOCD* overexpression in control VSMCs significantly reduced LRP protein levels ($P < 0.01$, Fig. 2d) and *LRP* mRNA transcripts by more than 80% (Fig. 2e), resulting in decreased Aβ clearance (Fig. 1c, e). Taken together, these data suggest that SRF and MYOCD control the Aβ clearance phenotype in VSMCs by regulating LRP expression at the transcriptional level.

SRF and MYOCD regulate LRP through SREBP-2

To delineate the molecular nature of SRF–MYOCD-mediated LRP suppression, we focused on SREBP2[23] because it is the only known transcriptional suppressor of LRP[24,25]. The human *SREBP2* promoter and intron 1 contain one and two CArG elements, respectively (Fig. 3a). MYOCD and SRF had no significant effect on the *SREBP2* promoter alone, but they activated it in the presence of intron 1 sequences in cultured VSMCs. Moreover, mutation of both CArG boxes in the intron 1 sequence ablated SRF and MYOCD activation of SREBP2 (Fig. 3a), suggesting that the observed activation of SREBP2 is CArG-dependent.

Next we studied whether increased SRF/MYOCD expression in cerebral VSMCs derived from AD individuals with CAA is associated with SREBP2 activation. We found that nuclear levels of SREBP2 are elevated in AD VSMC, compared with age-matched control VSMCs, which correlates with reduced LRP cellular expression, compared with controls (Fig. 3b versus d). Increased SREBP2 nuclear expression and decreased LRP expression in cultured cerebral

VSMCs from AD patients with CAA were consistent with findings demonstrating increased SREBP2 nuclear expression and reduced LRP expression in cerebral VSMC in AD leptomeningeal vessels *in situ*, relative to controls (Supplementary Information, Fig. S1f, g).

Nuclear levels of SREBP2 were downregulated and LRP levels increased in AD VSMC transduced with Ad.sh*SRF*, but not with Ad.sh*GFP* (Fig. 3b), as one would expect with removal of the LRP transcriptional suppressor[24,25]. Quantification of nuclear SREBP2 signal intensity and LRP cellular signal intensity after Ad.sh*SRF* transduction confirmed significant reductions in nuclear SREBP2 and increases in LRP expression (Supplementary Information, Fig. S2a). Western blot analysis confirmed that levels of both SREBP2 cytoplasmic long form and short nuclear form were reduced, and LRP expression increased in AD VSMC transduced with Ad.sh*SRF*, compared with Ad.sh*GFP* cells (Fig. 3c).

As expected, overexpression of *MYOCD* in control VSMCs upregulated SREBP2 long form, followed by increases in the level of SREBP2 short nuclear form and decreases in LRP cellular levels (Fig. 3d; Supplementary Information, Fig. S2b). This was confirmed by western blot analysis (Fig. 3e). Consistent with increased SREBP2 transcriptional activity, there was an increase in the expression of other SREBP2 target genes[23], such as *LDLR* (data not shown). Overexpression of *MYOCD* significantly upregulated SRF levels (Fig 1d, Fig 3e). To establish that MYOCD and SRF regulate LRP through SREBP2, we studied LRP expression in control VSMCs transduced with Ad.*MYOCD* and co-transfected with a short interfering RNA against *SREBP2* (*SREBP2* siRNA) or a control siRNA (si*CNTRL*), which does not cause specific degradation of any known cellular mRNA. VSMCs expressing si*CNTRL* and Ad.*MYOCD*, but not Ad.*GFP*, showed increased levels of SREBP2 precursor cytoplasmic form and its active form, and reduced LRP levels (Fig. 3f). In contrast, silencing SREBP2 with si*SREBP2* resulted in loss of LRP suppression after Ad.*MYOCD* gene transfer (Fig. 3f). Silencing SREBP2, but not si*CNTRL*, prevented loss of *LRP* mRNA levels after Ad.*MYOCD* gene transfer (Fig. 3g). These data indicate that downregulation of LRP by SRF and MYOCD requires an intermediate step, namely SRF–MYOCD transactivation of SREBP2.

Myocd suppresses LRP in mouse pial arteries

We next asked whether altering Srf and Myocd expression in cerebral VSMCs *in vivo* influences Aβ accumulation in vessels and focally in the brain of control mice and in mouse models of AD. As genetic inactivation of *Myocd* or *Srf* is embryonic lethal[27,32] and *Srf* overexpression results in severe cardiac abnormalities and death[33], we used adenoviral-mediated *MYOCD* or sh*SRF* gene transfer to mouse pial cerebral arteries using a subarachnoid cerebrospinal fluid perfusion technique[22]. Levels of MYOCD and SRF levels were higher in cerebral VSMCs *in situ* isolated from the sites of transduction with Ad.*MYOCD*, compared with Ad.*GFP* (Fig. 4a, b). MYOCD-transduced vessels expressed increased levels of VSMC-specific genes, for example, smooth muscle α-actin and calponin (Fig. 4a, b), as reported previously[22], demonstrating effective *MYOCD* gene transfer into the VSMC layer. Vessels transduced with Ad.*MYOCD* expressed 2.2-fold higher levels of the long form of SREBP2 and 90% lower levels of LRP, compared with GFP controls (Fig. 4a, b). Nuclear localization of SREBP2 and substantial downregulation of LRP after MYOCD *in vivo* gene transfer to pial vessels were confirmed by immunocytochemical staining (Fig. 4c). Moreover, *MYOCD* gene transfer increased levels of mouse endogenous Aβ42 in transduced subarachnoid pial vessels and focally in brain tissue by 3-fold and 70%, respectively (Fig. 4d, e), demonstrating an inhibition of Aβ clearance *in vivo*. Aβ40 levels were similarly increased (data not shown).

SRF and MYOCD influence Aβ pathology in AD mice

Next, we tested our hypothesis in a mouse model of CAA expressing the Dutch and Iowa vasculotropic *APP* mutations[11] and in the *APPsw*$^{\pm}$ mice, which develop significant CAA after

12 months of age[34]. The Dutch/Iowa mice accumulate Aβ in the brain earlier than *APPsw*$^{\pm}$ mice in spite of extremely low-level expression of human *APP* mutant in the brain[11]. In these mice Aβ clearance across the BBB is non-functional, leaving the perivascular arterial route as a key mechanism for Aβ drainage[12]. As cerebral VSMCs contribute to Aβ elimination during its drainage along the perivascular arterial route[2], we hypothesized that silencing *Srf* in neocortical pial arteries may improve focal Aβ clearance. Local transduction of cerebral pial vessels with Ad.sh*SRF*, compared with Ad.sh*GFP*, in 24-month-old Dutch/Iowa *APP* mice significantly reduced Aβ load in the transduced vessels area as well as focally in the underlying brain tissue, and decreased total amyloid load and Aβ40 and Aβ42 levels focally in brain (Fig. 5a–e). SREBP2 cytoplasmic and nuclear forms were downregulated more than 2.5-fold, and the relative abundance of immature LRP-600 and mature LRP-85 bands increased by about 4-fold in pial vessels transduced with Ad.sh*SRF*, compared with Ad.sh*GFP* vessels (Fig. 5f), suggesting increased *de novo* synthesis of LRP. These findings corroborated our findings in cultured human cerebral VSMCs (Fig. 2). Moreover, Ad.sh*SRF* transfer to pial vessels in 16-month-old *APPsw*$^{\pm}$ mice, compared with Ad.sh*GFP* controls resulted in a significant reduction of Aβ cerebrovascular load as demonstrated by a 5-day longitudinal 2-photon *in vivo* imaging of the cortical lamina I–III with methoxy-XO4 for amyloid and Texas Red dextran angiography (Fig. 5g). Aβ40 and 42 levels were also significantly reduced in the brain areas containing pial vessels transduced with Ad.sh*SRF*, compared with Ad.sh*GFP* (Fig. 5h). These findings suggest that *Srf* silencing in cerebral blood vessels increases local Aβ clearance *in vivo* and attenuates CAA in two models of familial AD, presumably by normalizing SREBP2 levels and alleviating the transcriptional brake on LRP expression.

In contrast, *MYOCD* gene transfer to pial cerebral vessels in 15-month-old Dutch/Iowa *APP*-expressing mice substantially increased Aβ40 and Aβ42 levels and Aβ load in the transduced vessel area and focally in brain tissue (Fig. 6a–c). Exacerbation of CAA was confirmed by thioflavin S-positive staining for fibrillar amyloid (Fig. 6d). *MYOCD* gene transfer significantly increased the levels of MYOCD and SRF (data not shown) and SREBP2 in transduced vessels, eliminated the mature LRP-85 band and reduced the levels of immature LRP-600 by more than 50%[12] (Fig. 6e). Transcriptional activity of SREBP2 was confirmed by increased expression of *LDLR* (data not shown), one of the SREBP2 target genes[23]. These data suggest that MYOCD and SRF activate SREBP2, and repress *de novo* synthesis of LRP in cerebral vessels *in vivo*, similarly to that as shown in human cerebral VSMCs *in vitro* (Fig. 2). We also showed that *MYOCD* gene transfer to neocortical pial vessels in 16-month-old *APPsw*$^{\pm}$ mice significantly ($P < 0.01$) increased Aβ40 and 42 levels, Aβ load and thioflavin S staining in pial arteries, Aβ40 and 42 levels, and Aβ load focally in brain (Supplementary Information, Fig. S3).

Hypoxia increases MYOCD expression

Neither oxidant stress nor Aβ accumulation are upstream of SRF and MYOCD[22]. Low levels of the mesenchyme homeobox gene-2 (*MEOX-2*) decrease LRP in brain endothelium of AD individuals[31], but *MEOX-2* does not regulate SRF/MYOCD in cerebral VSMCs[22]. Thus, we focused on our pilot observation suggesting that hypoxia increases *MYOCD* mRNA levels in VSMCs[22]. Cerebral hypoperfusion is a recurring feature in vascular and AD dementias, and hypoxia is a local cellular consequence of such reduced cerebral blood flow. Hypoxia (Fig. 7a) and/or co-transfection of normoxic VSMCs with the hypoxia-inducing factor-1α (HIF-1α; Fig. 7b), increased a MYOCD-driven *luciferase* promoter. Importantly, deletion of the hypoxia response element (HRE) abolished both hypoxia- and HIF-1α-induced *MYOCD* promoter activity (Fig. 7a, b). In cultured human VSMCs, hypoxia significantly increased *MYOCD* mRNA levels (Fig. 7c) and MYOCD and SRF protein levels by 6-fold, but reduced LRP expression (Fig. 7d). Consistent with these findings we found an increase in nuclear SREBP2 levels associated with decreased LRP expression when VSMCs were exposed to hypoxia (Fig. 7e). We then subjected 5–6-month-old *APPsw*$^{\pm}$ mice to a hypoxia chamber (10% to 8%

oxygen) for 2 weeks and found a significant increase in MYOCD and SRF levels in the pial blood vessels, as well as increased nuclear levels of SREBP2 and decreased LRP levels (Fig. 7f). Hypoxia increased the *MYOCD* mRNA levels by about 6-fold and reduced *LRP* mRNA levels by more than 60% (Fig. 7g). These changes in the molecular profile of pial vessels in *APPsw*$^{\pm}$ mice exposed to hypoxia were accompanied by increased Aβ40 and Aβ42 levels in these vessels, compared with normoxic control *APPsw*$^{\pm}$ mice (Fig. 7h). Silencing *SRF* resulted in normalization of Aβ cerebrovascular clearance (data not shown). Collectively, these findings provide the first molecular insight into how *MYOCD* gene regulation may occur in a pathophysiological setting and suggest that hypoxia represents a key environmental stimulus for AD VSMC-associated increases in SRF–MYOCD and the attending hypercontractility[22] and faulty Aβ clearance.

DISCUSSION

In this report, we advance the concept that SRF and MYOCD overexpression in cerebral VSMC may contribute to neurovascular dysfunction and dementia in AD by inducing a hypercontractile phenotype in small cerebral arteries, resulting in reduced cerebral blood flow [22], and by promoting an Aβ non-clearing VSMC phenotype through directed expression of SREBP2, which suppresses LRP, a key Aβ clearance receptor, resulting in the development of CAA and multifocal brain Aβ accumulations (Fig. 8a, b).

New roles for SRF and MYOCD have been described recently. MYOCD acts as a potent repressor of MyoD-mediated skeletal muscle cell differentiation in an SRF-CArG element independent manner[35]. SRF regulates neuronal migration and axon guidance[36] and learning[37]. The present study demonstrates that MYOCD and SRF mediate a CArG-dependent transcriptional switch in the cerebral VSMCs, controlling CAA and brain clearance of Aβ. This transcriptional switch needs both MYOCD and SRF and is unique to cerebral VSMCs, as MYOCD has not been found in brain endothelial cells or astrocytes and/or neuronal lineages.

The role of LRP as an Aβ clearance receptor on VSMC, as shown in the present study, is consistent with its reported role as an endocytic cargo receptor[38]. Impaired LRP-mediated clearance of Aβ in VSMCs in AD and AD models is consistent with reports demonstrating diminished LRP-mediated Aβ clearance at the BBB in AD and AD models[12,14,17,30,39]. In addition, soluble LRP in plasma provides a key endogenous peripheral ‘sink’ for Aβ in humans, which is impaired in AD[40].

SREBP2 negatively regulates LRP expression by binding to the sterol responsive element 1 site on the *LRP* gene[24]. SREBP2 is important in cholesterol homeostasis because it is specific for cholesterogenic genes[23]. By downregulating LRP, SREBP2 prevents LRP-mediated accumulation of intracellular cholesterol esters in macrophages and VSMCs[25]. Curiously, small pial and intracerebral arteries in AD do not accumulate aggregated LDL and cholesterol esters or develop atherosclerosis[1,2] possibly due to downregulated LRP[25]. Earlier work with truncated versions of SREBPs has shown that when cells express these truncated proteins the SREBP-dependent genes cannot be suppressed by sterols[41,42]. Similarly, in the presence of SRF–MYOCD-directed expression of SREBP2 in VSMCs, changes in sterol levels would not be expected to influence SREBP2 and/or SREBP2-dependent LRP expression.

Previous studies have shown that people chronically treated with cholesterol-lowering drugs, such as statins, are less prone to develop AD[43,44]. We reported that statins can increase LRP expression in vascular cells in the presence of Aβ[45], suggesting that LRP can escape SREBP2-mediated repression through a mechanism(s) outside the sterol-SREBP2 axis. On the basis of the present findings, it is likely that statins, particularly those that do not cross the BBB, may produce beneficial effects in AD, primarily through their action on blood vessels and

improvement of brain perfusion rather than by directly affecting cholesterol levels in the brain, to reduce Aβ production through the cholesterol-mediated pathway[46] and/or blockade of isoprenoid-mediated pathway[47]. It is also possible that organization of cerebral vessels in certain brain areas contributes to spatial restriction of amyloid accumulation in AD, preferentially affecting some areas, such as the entorhinal cortex.

Brains of AD patients are chronically hypoperfused and exposed to hypoxia[1,2,48,49]. Our findings in hypoxic cerebral VSMCs and in *APPsw*$^{\pm}$ mice subjected to hypoxia raise the possibility that hypoxia may be an initial stimulus for MYOCD upregulation and subsequent elevations in SRF in VSMC of AD patients and models. This is consistent with earlier reports suggesting that hypoxia increases the levels of MYOCD mRNA in cultured VSMC[22,50]. Thus, hypoxia can set in motion the SRF–MYOCD pathogenic pathway in AD specifically in VSMCs by upregulating MYOCD, whose expression in brain is restricted to VSMCs. Such increases in MYOCD may activate SRF, whose promoter region is controlled by two CArG elements[19].

In summary, we suggest that elevated SRF and MYOCD activity enhances Aβ accumulation in the vessel wall and this may initiate the development of CAA, focal Aβ brain accumulations, cerebral arterial hypoperfusion and neurovascular uncoupling, commonly seen in AD. Thus, SRF and MYOCD could be therapeutic targets for CAA associated with cognitive decline and impaired clearance of Aβ from the brain.

METHODS

AD individuals and controls

Cerebral VSMCs were isolated from small intracerebral and leptomeningeal arteries (Brodmann's areas 9/10) from late-stage AD individuals with CAA and non-demented age-matched controls with little or no pathology and without CAA. For clinical and neuropathological characteristics see Supplementary Information, Table S1.

Human VSMC culture

Pial arterial VSMCs were isolated and characterized as reported previously[22]. We used primary early passage 1 VSMCs.

Adenoviral sh.*SRF* and *MYOCD* gene constructs

Adenoviral sh*SRF* and *MYOCD* gene constructs were as we previously reported[22].

Adenoviral sh.*LRP* construct

The *LRP* RNAi gene construct was cloned into the BLOCK iT U6 RNAi expression entry vector.

Gene transfer to VSMC

This was performed as reported previously[22].

Cellular clearance of Aβ deposits

The multi-spot glass slides were coated with Cy3-labelled Aβ42 or Aβ40 (ref. 26) at 5^μg per spot without cells, with control cerebral VSMCs or AD VSMCs, AD VSMCs transduced with Ad.sh*SRF* or Ad.sh*GFP*, or control VSMCs transduced with Ad.*MYOCD* or Ad.*GFP*. Cells (2,500 per spot) were incubated for 5 days in DMEM containing 10% heat-inactivated FBS, penicillin and streptomycin (Invitrogen). Cells were labelled with Cell Tracker Green CMFDA (Invitrogen C7025) and Lysotracker Blue DND-22 then fixed with 4% paraformaldehyde.

Images were scanned using a Zeiss 510 meta multi-photon/confocal microscope with a 543 nm HeNe laser to detect Cy3-Aβ42, a 488 nm Argon laser to detect Cell Tracker Green and an 800-nm tuned Ti:sapphire Laser (Mai Tai Spectra Physics) to detect Lyostracker Blue. Twenty randomly chosen spots per slide from 3–4 independent cultures per group were analysed. The relative Cy3 signal intensity was measured with the NIH Image J software.

QPCR for LRP mRNA in cultured VSMC

QPCR was performed using SYBR Green (Bio-Rad) and the Stratagene MX3005P QPCR system.

SREBP2 luciferase reporter assay

We cloned from HeLa genomic DNA the human SREBP2 promoter (1,375 bp encompassing one CArG element) and intron 1 sequences (1,315 bp encompassing 2 CArG elements) for responsiveness to SRF/MYOCD. Following sequence validation, we cloned the *SREBP2* promoter into the pGL3 basic vector (Promega) either alone or in combination with the intronic sequence. Mutations in the *SREBP2* CArG elements were performed with a QuikChange mutagenesis kit (Stratagene) where the first 3 nucleotides of the CArG element were changed to GTC. Luciferase activity was measured using a Dual-Luciferase Reporter Assay System (Promega) and normalized to a control (Renilla) vector.

SREBP2 knockdown in cultured human VSMCs

Control siRNA (si*CNTRL*, Santa Cruz, sc-37007) or *SREBP2* siRNA (sc-36559) were transfected into cultured VSMCs using Metafectene (Biontex) according to the manufacturer's instruction.

Western blotting

Expression of SRF, MYOCD, SREBP2 and LRP was studied by western blot analysis in human cerebral VSMCs and small cerebral leptomenigeal arteries (Brodmann's areas 9/10) derived from AD patients with CAA and controls. VSMC samples were washed in cold phosphate buffer saline and lysed with a RIPA buffer. Small cerebral arteries samples were additionally sonicated in the RIPA buffer. Proteins were quantified with a protein assay kit (Pierce).

Immunostaining for nuclear SREBP2 and LRP

AD VSMCs infected with Ad.sh*GFP* or Ad.sh*SRF* or control VSMCs infected with Ad.*LacZ* or Ad.*MYOCD* were cultured for 48 h and fixed in 4% paraformaldehyde. Cells and human brain sections (Brodmann's area 9/10) were then stained using a rabbit anti-human SREBP2 antibody (Abcam, ab30682) and mouse anti-human LRP (Calbiochem, 438192) followed by incubation with secondary antibodies, such as FITC-conjugated goat and rabbit, CY3 conjugated donkey anti-mouse and TO-PRO3, a fluorescent nuclear marker (Invitrogen). Cells and tissue were scanned using a Zeiss 510 meta multi-photon/confocal microscope with a 543-nm HeNe laser to detect Cy3, a 488-nm Argon laser to detect FITC, a 633-nm HeNe laser to detect TO-PRO3, and an 800-nm tuned Ti:sapphire Laser (Mai Tai Spectra Physics) to detect methoxy-X04.

MYOCD *luciferase* reporter assay

We cloned the mouse *Myocd* promoter from genomic DNA with or without the conserved hypoxia response element (HRE). Following sequence validation, we cloned the MYOCD promoters into the pGL3 basic vector (Promega). PAC1 VSMC were transfected with *luciferase* reporters, then incubated in DMEM containing 2% FBS under normoxic (21% oxygen) or hypoxic (1% oxygen) conditions, or co-transfected with either control or HIF1α

expression plasmid construct (gift from Gregg Semenza, Johns Hopkins, MD). Human control VSMCs were incubated in DMEM containing 2% FBS under either normoxic (21% O_2) or hypoxic (1% O_2) conditions.

Transgenic mice

Dutch/Iowa *APP* transgenic mice[11] at 24 months of age and *APPsw*$^{\pm}$ mice[34] at 16 months of age were used to silence *Srf*. Dutch/Iowa *APP*[11] at 15 months of age and *APPsw*$^{\pm}$ mice at 16 months of age were used to overexpress *Myocd*. All procedures with animals have been preformed using an approved institutional protocol according to the NIH guidelines.

In vivo transduction of cerebral pial arteries

This procedure was performed as we reported previously[22].

Aβ levels after *in vivo* gene transfer

We determined endogenous Aβ40 and Aβ42 levels in the vessels and focally in brain tissue in control mice by a sandwich ELISA, as reported previously[40].

The levels of human Aβ40 and Aβ42 in the Dutch/Iowa *APP* mice and *APPsw*$^{\pm}$ mice were determined using ELISA kits KHB3481 and KHB3441, respectively (Biosource), as we reported previously[40]. In all studies, Aβ levels were determined focally in brain parenchyma.

Aβ immunostaining of brain tissue in Dutch/Iowa *APP* and *APPsw*$^{\pm}$ mice

Cyrostat sections (10 μm) were stained using polyclonal anti-pan Aβ (1:200; Invitrogen, 44–136) and polyclonal anti-mouse CD31 (1:200; BD Pharmingen, 550274). Fluorescence imaging was obtained using fluorescein goat anti-rabbit IgG (1:200; Invitrogen, F-2765) and Alexa Fluor 594 donkey anti-rat IgG (1:200; Invitrogen, A-21209).

Thioflavin S amyloid staining

Sections were incubated in 0.5% thioflavin S in 70% ethanol for 5 min and washed with distilled water.

Western blotting of isolated brain vessels

Vessels were washed with PBS and lysed with a buffer as above. MYOCD, SRF, SREBP2, LRP and β-actin were detected using the primary antibodies as described above. Primary antibodies for SM-calponin (1:10,000, hCP, Sigma) and SM α-actin (1:1,000, Sigma, A-2547) were also used. Quantification was performed by densitometry analysis using a AlphaImager 2200 and AlphaEase FC software (Alpha Innotech Corporation).

Immunostaining for SREBP2 and LRP in MYOCD-transduced vessels in control mice

Five days after *GFP* or *MYOCD* gene transfer, 10-μm frozen sections of brain were stained for SREBP2 nuclear localization and LRP as described above.

Multiphoton *in vivo* imaging of CAA

We performed a longitudinal 5-day multiphoton *in vivo* imaging of vascular amyloid in 16-month-old *APPsw*$^{\pm}$ mice transduced with Ad.sh*SRF* or Ad.sh*GFP*. Imaging was perfomed on the day of transduction and 5 days after transduction. One day before imaging, animals received an intraperitoneal injection of 10 mg kg^{-1} methoxy-X04 (Neuroptix). For imaging, mice were anaesthetized with urethane (750 mg kg^{-1}, i.p.) and chloralose (50 mg kg^{-1}, i.p.). Texas Red conjugated Dextran (70K; 200 mg kg^{-1}) was injected into the tail vein to create a fluorescent angiogram. *In vivo* images were acquired using a Zeiss 5MP multi-photon microscope coupled

to a 900-nm mode locked Ti:sapphire laser (Mai Tai, Spectra Physics). Quantification of residual X-04 fluorescence was analysed using NIH Image J software.

In vivo hypoxia model

We used a normobaric chamber with 10% oxygen on the first day, 9% on the second day, and then 8% of oxygen for up to 2 weeks, as we described previously[31].

Statistical analysis

ANOVA was used to determine statistically significant differences. $P < 0.05$ was considered statistically significant.

ACKNOWLEDGEMENTS

We thank Ms. Theresa Barrett for assisting with some immunostaining studies. This study was supported by R37AG023084, R37NS34467 and Socratech LLC to BVZ, 1R43 AG02400 to NC and HL62572 and R42AG026950 to JMM. JMM and BVZ are co-senior authors.

References

1. Iadecola C. Neurovascular regulation in the normal brain and in Alzheimer's disease. Nature Rev. Neurosci 2004;5:347–360. [PubMed: 15100718]
2. Zlokovic BV. The blood-brain barrier in health and chronic neurodegenerative disorders. Neuron 2008;57:178–201. [PubMed: 18215617]
3. Tanzi RE, Moir RD, Wagner SL. Clearance of Alzheimer's Abeta peptide: the many roads to perdition. Neuron 2004;43:605–608. [PubMed: 15339642]
4. Haass C, Selkoe DJ. Soluble protein oligomers in neurodegeneration: lessons from the Alzheimer's amyloid beta-peptide. Nature Rev. Mol. Cell Biol 2007;8:101–112. [PubMed: 17245412]
5. Greenberg SM, Gurol ME, Rosand J, Smith EE. Amyloid angiopathy-related vascular cognitive impairment. Stroke 2004;35:2616–2619. [PubMed: 15459438]
6. Jellinger KA. Alzheimer disease and cerebrovascular pathology: an update. J. Neural Transm 2002;109:813–836. [PubMed: 12111471]
7. Pettersen JA, et al. Microbleed topography, leukoaraiosis, and cognition in probable Alzheimer disease from the Sunnybrook Dementia Study. Arch. Neurol 2008;65:790–795. [PubMed: 18541799]
8. Zlokovic BV, Yamada S, Holtzman D, Ghiso J, Frangione B. Clearance of amyloid beta-peptide from brain: transport or metabolism? Nature Med 2000;6:718–719.
9. Selkoe DJ. Clearing the brain's amyloid cobwebs. Neuron 2001;32:177–180. [PubMed: 11683988]
10. Holtzman, DM.; Zlokovic, BV. Role of Aβ transport and clearance in the pathogenesis and treatment of Alzheimer's disease. In: Sisodia, SS.; Tanzi, RE., editors. Alzheimer's Disease: Advances in Genetics, Molecular and Cellular Biology. New York: Springer; 2007. p. 179-198.
11. Davis J, et al. Early-onset and robust cerebral microvascular accumulation of amyloid beta-protein in transgenic mice expressing low levels of a vasculotropic Dutch/Iowa mutant form of amyloid beta-protein precursor. J. Biol. Chem 2004;279:20296–20306. [PubMed: 14985348]
12. Deane R, et al. LRP/amyloid beta-peptide interaction mediates differential brain efflux of Abeta isoforms. Neuron 2004;43:333–344. [PubMed: 15294142]
13. Kumar-Singh S, et al. Dense-core plaques in Tg2576 and PSAPP mouse models of Alzheimer's disease are centered on vessel walls. Am. J. Pathol 2005;167:527–543. [PubMed: 16049337]
14. Shibata M, et al. Clearance of Alzheimer's amyloid-ss(1–40) peptide from brain by LDL receptor-related protein-1 at the blood-brain barrier. J. Clin. Invest 2000;106:1489–1499. [PubMed: 11120756]
15. Moir RD, Tanzi RE. LRP-mediated clearance of Aβ is inhibited by KPI-containing isoforms of APP. Curr. Alzheimer Res 2005;2:269–273. [PubMed: 15974929]

16. Bell RD, et al. Transport pathways for clearance of human Alzheimer's amyloid beta-peptide and apolipoproteins E and *J*. in the mouse central nervous system. J. Cereb. Blood Flow Metab 2007;27:909–918. [PubMed: 17077814]

17. Nazer B, Hong S, Selkoe DJ. LRP promotes endocytosis and degradation, but not transcytosis, of the amyloid-beta peptide in a blood-brain barrier *in vitro* model. Neurobiol. Dis 2008;30:94–102. [PubMed: 18289866]

18. Urmoneit B, et al. Cerebrovascular smooth muscle cells internalize Alzheimer amyloid beta protein via a lipoprotein pathway: implications for cerebral amyloid angiopathy. Lab. Invest 1997;77:157–166. [PubMed: 9274858]

19. Miano JM. Serum response factor: toggling between disparate programs of gene expression. J. Mol. Cell. Cardiol 2003;35:577–593. [PubMed: 12788374]

20. Wang D, et al. Activation of cardiac gene expression by myocardin, a transcriptional cofactor for serum response factor. Cell 2001;105:851–862. [PubMed: 11439182]

21. Pipes GC, Creemers EE, Olson EN. The myocardin family of transcriptional coactivators: versatile regulators of cell growth, migration, and myogenesis. Genes Dev 2006;20:1545–1556. [PubMed: 16778073]

22. Chow N, et al. Serum response factor and myocardin mediate arterial hypercontractility and cerebral blood flow dysregulation in Alzheimer's phenotype. Proc. Natl Acad. Sci. USA 2007;104:823–828. [PubMed: 17215356]

23. Brown MS, Goldstein JL. The SREBP pathway: regulation of cholesterol metabolism by proteolysis of a membrane-bound transcription factor. Cell 1997;89:331–340. [PubMed: 9150132]

24. Llorente-Cortés V, Costales P, Bernués J, Camino-Lopez S, Badimon L. Sterol regulatory element-binding protein-2 negatively regulates low density lipoprotein receptor-related protein transcription. J. Mol. Biol 2006;359:950–960. [PubMed: 16697011]

25. Llorente-Cortés V, Royo T, Otero-Viñas M, Berrozpe M, Badimon L. Sterol regulatory element binding proteins downregulate LDL receptor-related protein (LRP1) expression and LRP1-mediated aggregated LDL uptake by human macrophages. Cardiovasc. Res 2007;74:526–536. [PubMed: 17376415]

26. Wyss-Coray T, et al. Adult mouse astrocytes degrade amyloid-beta *in vitro* and *in situ*. Nature Med 2003;9:453–457. [PubMed: 12612547]

27. Miano JM, et al. Restricted inactivation of serum response factor to the cardiovascular system. Proc. Natl Acad. Sci. USA 2004;101:17132–17137. [PubMed: 15569937]

28. Parlakian A, et al. Targeted inactivation of serum response factor in the developing heart results in myocardial defects and embryonic lethality. Mol. Cell. Biol 2004;24:5281–5289. [PubMed: 15169892]

29. Niu Z, et al. Conditional mutagenesis of the murine serum response factor gene blocks cardiogenesis and the transcription of downstream gene targets. J. Biol. Chem 2005;280:32531–32538. [PubMed: 15929941]

30. Donahue JE, et al. RAGE, LRP-1, and amyloid-beta protein in Alzheimer's disease. Acta. Neuropathol 2006;112:405–415. [PubMed: 16865397]

31. Wu Z, et al. Role of the MEOX2 homeobox gene in neurovascular dysfunction in Alzheimer disease. Nature Med 2005;11:959–965. [PubMed: 16116430]

32. Li S, Wang DZ, Wang Z, Richardson JA, Olson EN. The serum response factor coactivator myocardin is required for vascular smooth muscle development. Proc. Natl Acad. Sci. USA 2003;100:9366–9370. [PubMed: 12867591]

33. Zhang X, et al. Cardiomyopathy in transgenic mice with cardiac-specific overexpression of serum response factor. Am. J. Physiol. Heart Circ. Physiol 2001;280:H1782–H1792. [PubMed: 11247792]

34. Holtzman DM, et al. Apolipoprotein E facilitates neuritic and cerebrovascular plaque formation in an Alzheimer's disease model. Ann. Neurol 2000;47:739–747. [PubMed: 10852539]

35. Long X, Creemers EE, Wang DZ, Olson EN, Miano JM. Myocardin is a bifunctional switch for smooth versus skeletal muscle differentiation. Proc. Natl Acad. Sci. USA 2007;104:16570–16575. [PubMed: 17940050]

36. Alberti S, et al. Neuronal migration in the murine rostral migratory stream requires serum response factor. Proc. Natl. Acad. Sci. USA 2005;102:6148–6153. [PubMed: 15837932]

37. Etkin A, et al. A role in learning for SRF: deletion in the adult forebrain disrupts LTD and the formation of an immediate memory of a novel context. Neuron 2006;50:127–143. [PubMed: 16600861]
38. Herz J, Marschang P. Coaxing the LDL receptor family into the fold. Cell 2003;112:289–292. [PubMed: 12581519]
39. Herring A, et al. Environmental enrichment counteracts Alzheimer's neurovascular dysfunction in TgCRND8 Mice. Brain Pathol 2008;18:32–39. [PubMed: 17924982]
40. Sagare A, et al. Clearance of amyloid-beta by circulating lipoprotein receptors. Nature Med 2007;13:1029–1031. [PubMed: 17694066]
41. Sato R, et al. Assignment of the membrane attachment, *DNA* binding, and transcriptional activation domains of sterol regulatory element-binding protein-1 (SREBP-1). J. Biol. Chem 1994;269:17267–17273. [PubMed: 8006035]
42. Yang J, Brown MS, Ho YK, Goldstein JL. Three different rearrangements in a single intron truncate sterol regulatory element binding protein-2 and produce sterol-resistant phenotype in three cell lines. J. Biol. Chem 1995;270:12152–12161. [PubMed: 7744865]
43. Wolozin B, Kellman W, Ruosseau P, Celesia GG, Siegel G. Decreased prevalence of Alzheimer disease associated with 3-hydroxy-3-methyglutaryl coenzyme A reductase inhibitors. Arch. Neurol 2000;57:1439–1443. [PubMed: 11030795]
44. Sparks DL, et al. Atorvastatin for the treatment of mild to moderate Alzheimer disease: preliminary results. Arch. Neurol 2005;62:753–757. [PubMed: 15883262]
45. Deane R, Wu Z, Zlokovic BV. RAGE (yin) versus LRP (yang) balance regulates alzheimer amyloid beta-peptide clearance through transport across the blood-brain barrier. Stroke 2004;35:2628–2631. [PubMed: 15459432]
46. Puglielli L, et al. Acyl-coenzyme A: cholesterol acyltransferase modulates the generation of the amyloid beta-peptide. Nature Cell Biol 2001;3:905–912. [PubMed: 11584272]
47. Parsons RB, et al. Statins inhibit the dimerization of beta-secretase via both isoprenoid- and cholesterol-mediated mechanisms. Biochem. J 2006;399:205–214. [PubMed: 16803455]
48. Vermeer SE, et al. Silent brain infarcts and the risk of dementia and cognitive decline. N. Engl. J. Med 2003;348:1215–1222. [PubMed: 12660385]
49. Ruitenberg A, et al. Cerebral hypoperfusion and clinical onset of dementia: the Rotterdam Study. Ann. Neurol 2005;57:789–794. [PubMed: 15929050]
50. Zhu P, Huang L, Ge X, Yan F, Wu R, Ao Q. Transdifferentiation of pulmonary arteriolar endothelial cells into smooth muscle-like cells regulated by myocardin involved in hypoxia-induced pulmonary vascular remodeling. Int. J. Exp. Pathol 2007;87:463–474. [PubMed: 17222214]

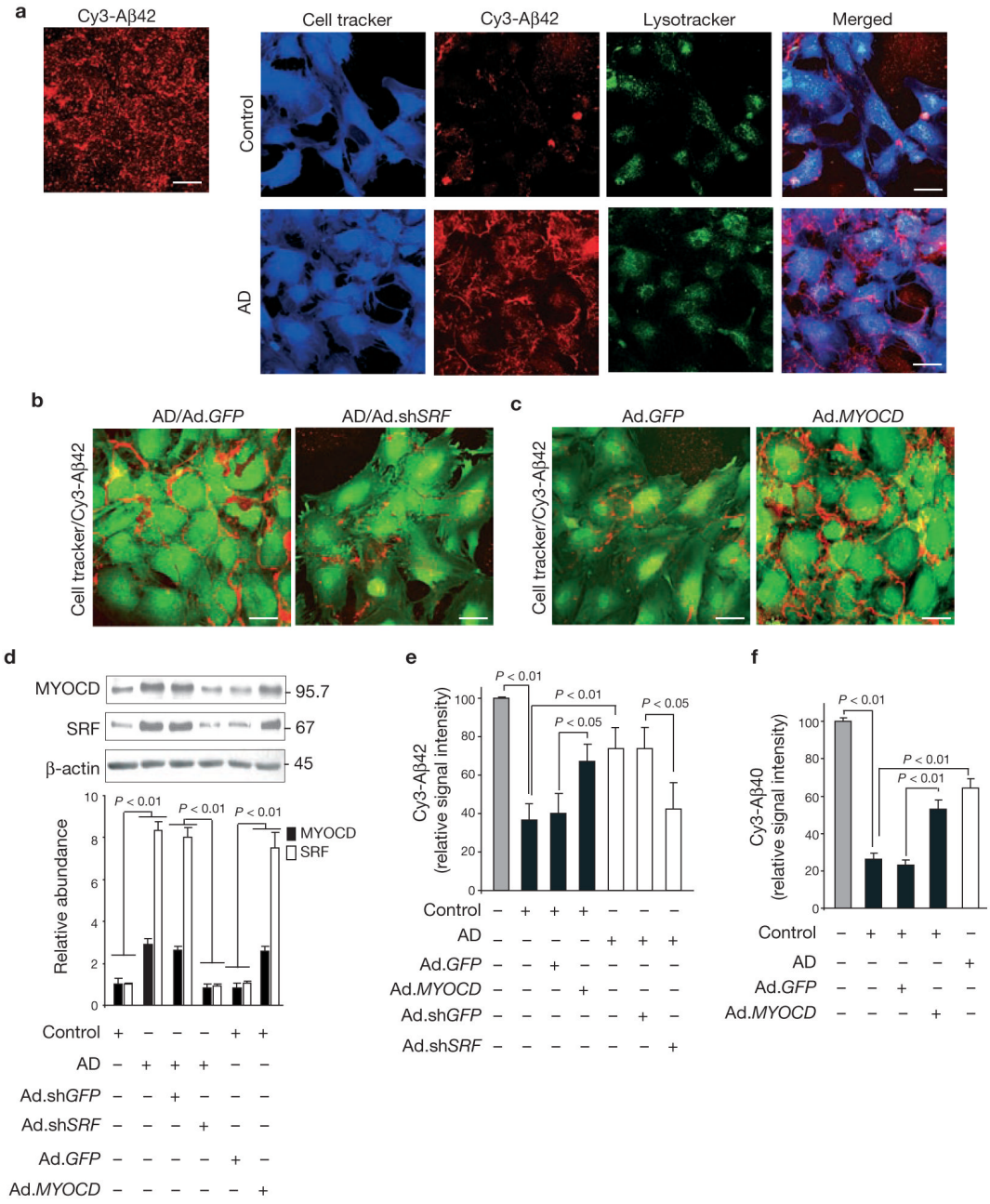

Figure 1.

SRF and MYOCD overexpression blocks Aβ clearance by human cerebral VSMCs. (**a**) Multi-photon/confocal laser scanning microscopy of multi-spot glass slides coated with Cy3-labelled Aβ42 without cells (left panel) and with cerebral VSMCs (right panels) from AD individuals and age-matched controls grown for 5 days. (**b**) VSMCs from AD individuals transduced with Ad.sh*GFP* or Ad.sh*SRF* at MOI 100, plated and grown on Cy3-Aβ42-coated surfaces for 5 days and imaged by confocal microscopy. (**c**) VSMC from controls transduced with Ad.*GFP* or Ad.*MYOCD* plated and grown on Cy3-Aβ42-coated surfaces for 5 days and imaged by confocal microscopy. Scale bars, 50 μm (**a–c**). (**d**) Western blots of SRF and MYOCD in AD and age-matched control VSMCs incubated with vehicle and transduced with

Ad.sh*GFP* and Ad.sh*SRF* or Ad.*GFP* and Ad.*MYOCD*, respectively. Relative levels of expression determined by scanning densitometry are shown below the blots (mean ± s.e.m. of 3–4 independent cultures). (**e**) Cy3-Aβ42 relative signal intensity on multi-spot slides after 5 days with control VSMCs, non-transduced or transduced with Ad.*GFP* or Ad.*MYOCD* (black bars), and with AD VSMC not transduced or transduced with Ad.sh*GFP* or Ad.sh*SRF* (open bars). Mean ± s.e.m. of 7–8 independent cultures are shown. (**f**) Cy3-Aβ40 relative signal intensity after 5 days in control VSMCs, non-transduced or transduced with Ad.*GFP* or Ad.*MYOCD* (black bars), compared with AD VSMCs (open bar). Mean ± s.e.m., from 3–4 independent cultures are shown. In **e** and **f**, the signal intensity in cell-free slides (grey bar) was arbitrarily taken as 100%. Full scans of western blot data are shown in Supplementary Information, Fig. S4.

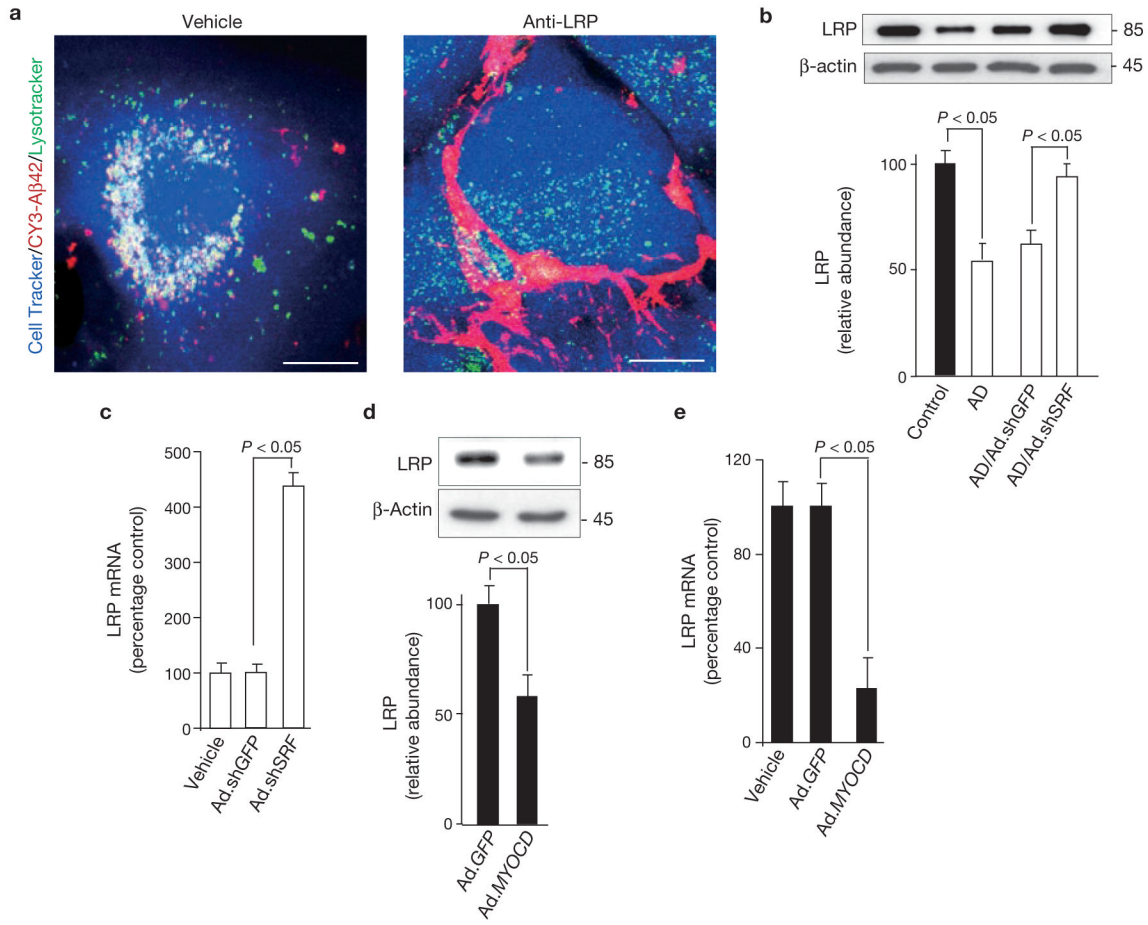

Figure 2.

LRP in cerebral VSMCs is downregulated by SRF and MYOCD. (**a**) Multi-photon/confocal laser scanning microscopy of Cy3-Aβ42 internalization and lysosomal colocalization in control VSMCs treated with vehicle and a LRP-specific blocking antibody. Cell Tracker, blue; Cy3-Aβ42, red; Lysotracker, green. Merged images are shown (yellow-white colour is colocalization of Aβ with lysosomes). Scale bar, 20 μm. (**b**) LRP levels in control and AD cerebral VSMCs, and in AD VSMCs transduced with Ad.sh*GFP* and Ad.sh*SRF*. (**c**) Real-time quantitative PCR (qPCR)for *LRP* mRNA in AD VSMCs alone (vehicle) and transduced with Ad.sh*GFP* or Ad.sh*SRF*. (**d**) LRP levels in control VSMC transduced with Ad.*GFP* or Ad.*MYOCD*. (**e**) Real-time qPCR for *LRP* mRNA in control VSMCs alone (vehicle) and transduced with Ad.*GFP* or Ad.*MYOCD*. Data represent mean ± s.e.m. of 3 independent cultures per group (**b–e**).

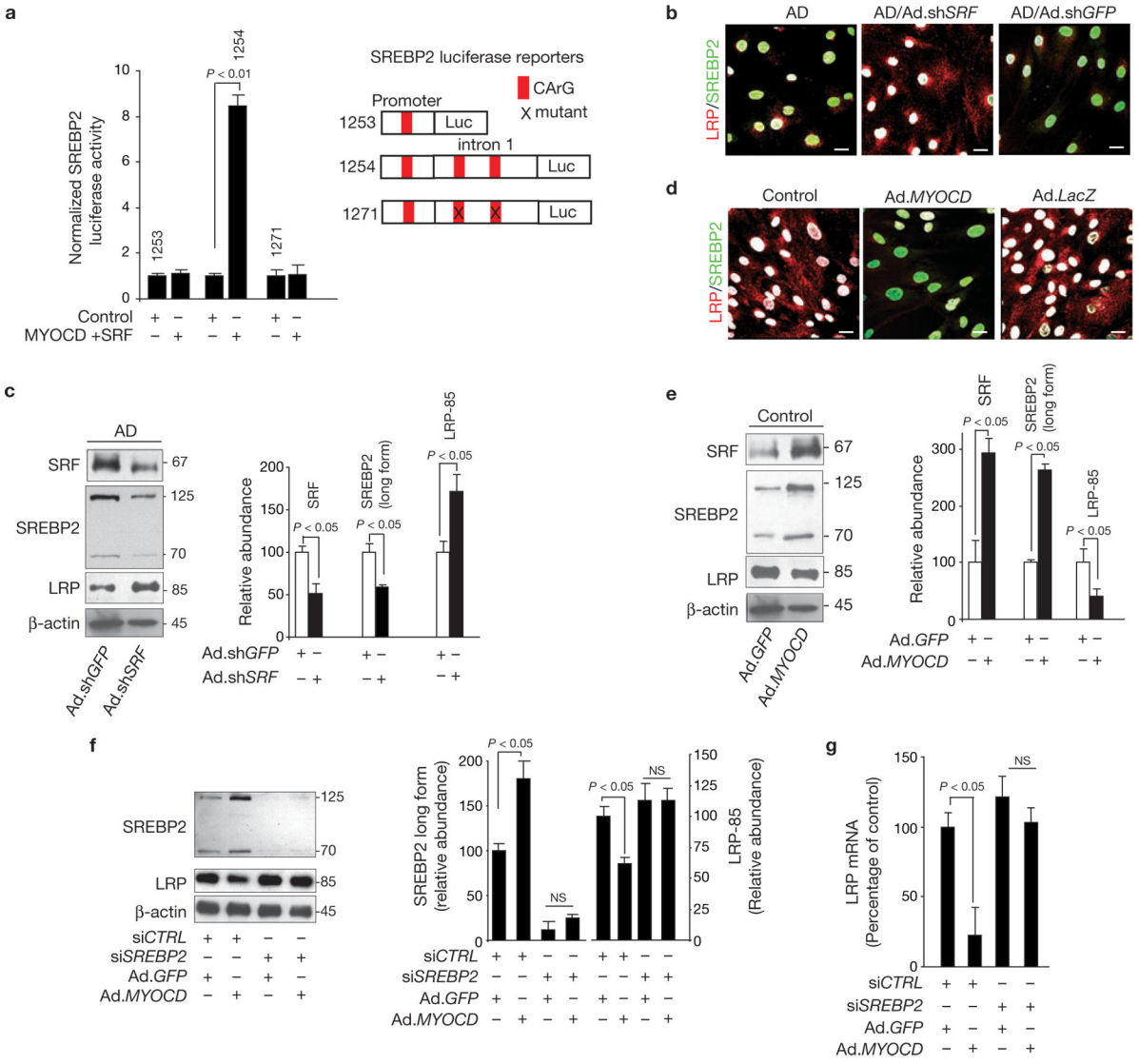

Figure 3.

SRF and MYOCD suppress LRP through directed expression of SREBP2. (**a**) SREBP2 luciferase activity in PAC1 VSMCs after co-transfection with a *luciferase* reporter containing the promoter (1253), promoter plus intron 1 (1254) or promoter plus intron 1 with both CArG boxes mutated (1271) of human SREBP2, with pcDNA vector and EMSV vector (control) or with MYOCD and SRF overexpression plasmids. (**b**) Increased levels of nuclear SREBP2 (green) and low cellular expression of LRP (red) in AD VSMCs, compared with control VSMC (see **d**). Reduced nuclear SREBP2 levels and increased LRP expression after transduction of AD VSMCs with Ad.sh*SRF* but not Ad.sh*GFP*. Nuclear DAPI staining is shown in white. Scale bar, 20 μm. (**c**) SRF, SREBP2 (cytoplasmic long form and short nuclear form) and LRP levels determined by western blot analysis in AD VSMC transduced with Ad.sh*GFP* and Ad.sh*SRF*. (**d**) Low levels of nuclear SREBP2 (green) and increased cellular expression of LRP (red) in control VSMCs, compared with AD VSMC (see **b**). Increased nuclear SREBP2 and reduced LRP expression after transduction of control VSMCs with Ad.*MYOCD*, but not with Ad.*GFP*. Nuclear DAPI staining in white. Scale bars, 20 μm. (**e**). SRF, SREBP2

(cytoplasmic long form and short nuclear form) and LRP levels determined by western blot analysis after transduction of control VSMCs with Ad.*GFP* or Ad.*MYOCD*. Graphs in **c** and **e** show band density relative to β-actin. (**f**) SREBP2 and LRP levels in control VSMC transfected with control siRNA (si*CTRL*) or *SREBP2* siRNA (si*SREBP2*) followed by transduction with either Ad.*GFP* or Ad.*MYOCD*. Graph shows band density for test-proteins relative to β-actin. (**g**) Real-time qPCR for *LRP* mRNA in control VSMCs transfected with control siRNA (si*CTRL*) or *SREBP2* siRNA (si*SREBP2*) followed by transduction with either Ad.*GFP* or Ad.*MYOCD*. Data represent mean ± s.e.m. of 9 independent cultures; values were normalized to an internal renilla control (**a**), or mean ± s.e.m. of 3 independent cultures per group (**c**, **e–g**). Full scans of western blot data in panel f are shown in Supplementary Information, Fig. S4.

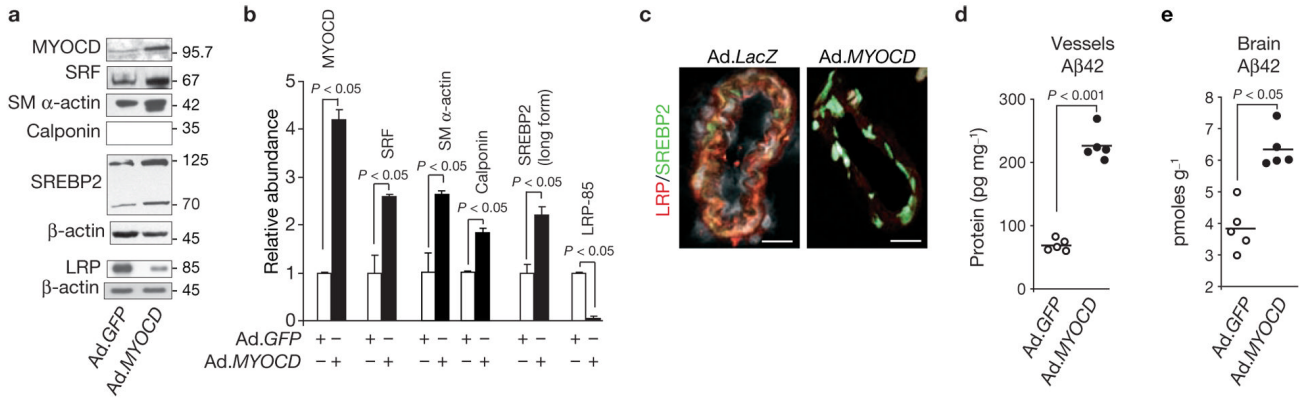

Figure 4.

MYOCD overexpression in pial arteries suppresses focal LRP-mediated Aβ clearance in mice. (**a**, **b**) MYOCD, SRF, smooth muscle α-actin, smooth muscle calponin, SREBP2 and LRP levels determined by western blotting in cerebral pial vessels isolated after *in vivo* transduction with Ad.*GFP* or Ad.*MYOCD* in 5-month-old C57Bl6 mice (**a**). Graph shows band density of test-proteins relative to β-actin (mean ± s.e.m. from 5 animals per group, **b**). (**c**) Immunocytochemical staining for nuclear SREBP2 and cellular LRP in pial vessels after *MYOCD* gene transfer. LRP, red; SREBP2, green; TO-PRO3, grey. Scale bars, 20 μm. (**d**, **e**) Effects of *MYOCD* overexpression on endogenous Aβ42 levels in mouse transduced pial vessels (**d**) and focally in brain (**e**). Each point represents an individual animal value. Full scans of western blot data are shown in Supplementary Information, Fig. S4.

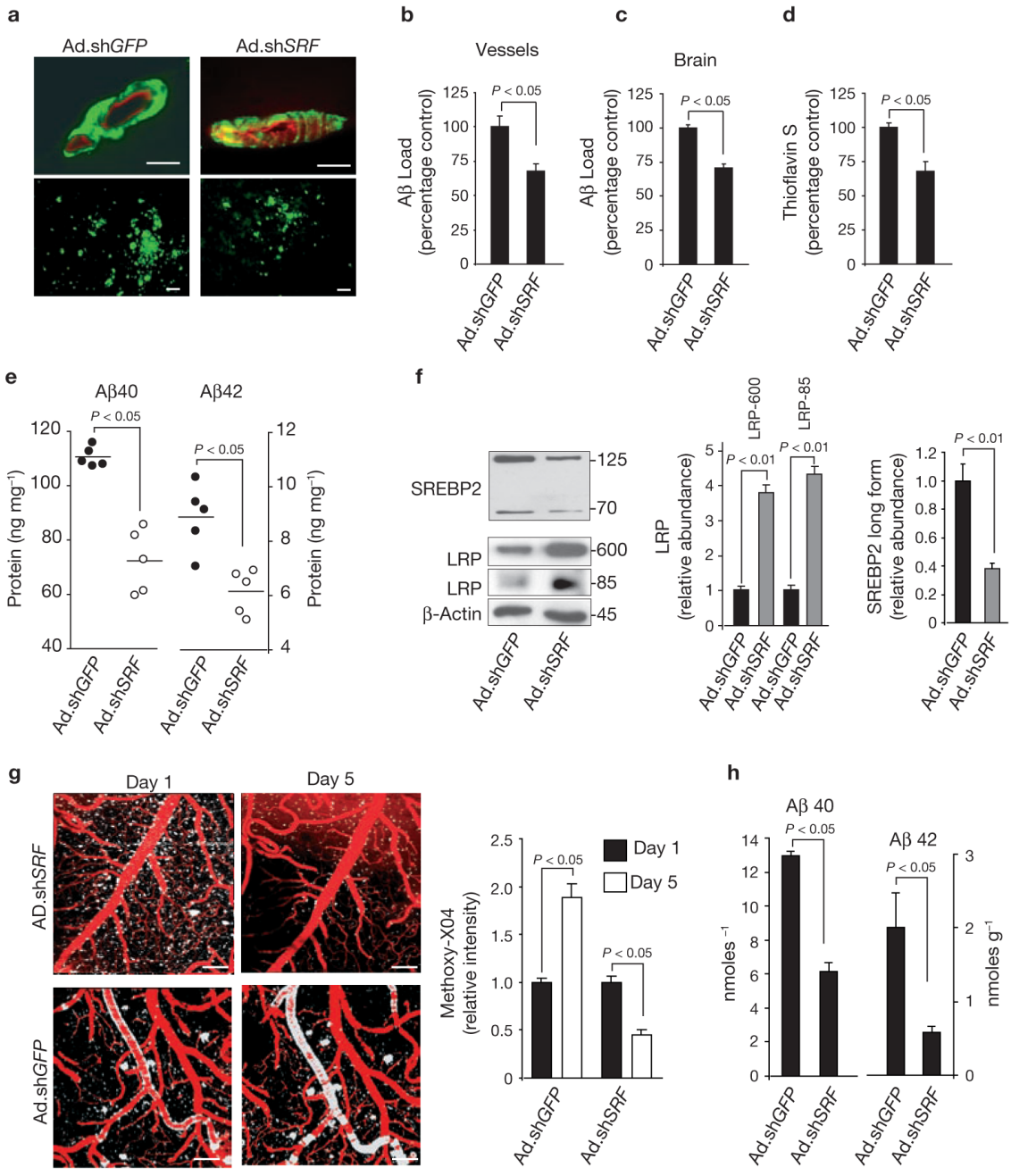

Figure 5.

SRF gene transfer to pial arteries reduces Aβ pathology in AD models. (**a**) Aβ immunostaining in transduced pial vessels (upper panels) and focally in brain tissue (lower panels) after expression of a control vector (Ad.sh*GFP*) or Ad.sh*SRF* in 24-month-old Dutch/Iowa *APP* mice. Scale bars,50 μm. (**b**, **c**) Aβ load in transduced pial vessels (**b**) and focally in brain (**c**) after adenoviral-mediated transfer of sh*GFP* or sh*SRF* in 24-month-old Dutch/Iowa *APP* mice. (**d**, **e**) Amyloid load in transduced pial vessels (**d**) and focal Aβ40 and Aβ42 levels in brain (**e**) after adenoviral-mediated transfer of sh*GFP* and sh*SRF* in 24-month-old Dutch/Iowa *APP* mice. (**f**) The levels of SREBP2, immature LRP (LRP 600 band) and mature LRP (LRP 85 band) in pial vessels after overexpression of sh*GFP* and sh*SRF* in 24-month-old Dutch/

Iowa *APP* mice. Graphs show relative band density, compared with β-actin. (**g**) 2-photon *in vivo* longitudinal imaging of amyloid with methoxy-XO4 and Texas Red dextran angiography in the cortical lamina I in 16-month-old *APPsw*$^{\pm}$ mice transduced locally in the pial vessels with either Ad.sh*GFP* or Ad.sh*SRF*. Scale bars, 100 μm. Graphs show XO4 relative signal intensity. (**h**) Aβ40 and Aβ42 focal brain levels in the areas containing pial vessels transduced with Ad.sh*GFP* or Ad.sh*SRF* in 16-month-old *APPsw*$^{\pm}$ mice. Data represent mean ± s.e.m. of 5 animals per group (**b–d**, **f–h**).

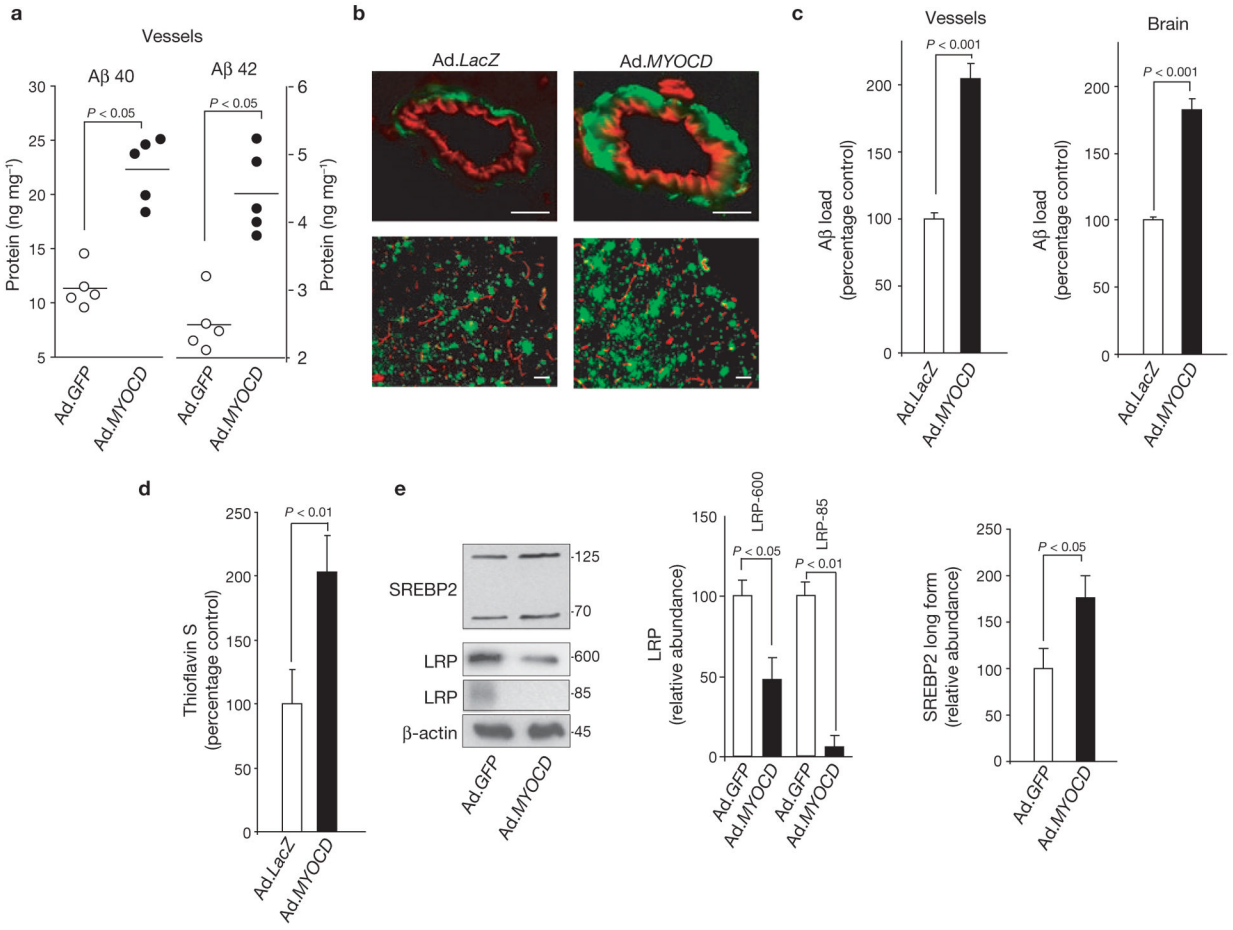

Figure 6.

MYOCD overexpression in pial arteries aggravates Aβ pathology in the Dutch/Iowa *APP* mice. (**a**) Aβ40 and Aβ42 levels in the pial vessels after transfer of Ad.*GFP* and Ad.*MYOCD*. Each point represents an individual value. (**b**) Aβ immunostaining in transduced pial vessels (upper panels) and focally in brain tissue (lower panels) after expression of a control vector (Ad.*LacZ*) or Ad.*MYOCD*. Scale bars, 50 μm. (**c**) Aβ load in transduced pial vessels and focally in brain after transfer of Ad.*LacZ* or Ad.*MYOCD*. (**d**) Amyloid load in pial vessels after transduction of Ad.*LacZ* or Ad.*MYOCD*. (**e**) The levels of SREBP2 long and short forms, immature LRP (LRP 600 band) and mature LRP (LRP 85 band) in pial vessels after overexpression of *GFP* and *MYOCD*. Graph shows relative band density, compared with β-actin. Data represent mean ± s.e.m. of 5 animals per group (**c–e**). *MYOCD* and *GFP* gene transfer was performed in 15-month-old Dutch/Iowa *APP* mice.

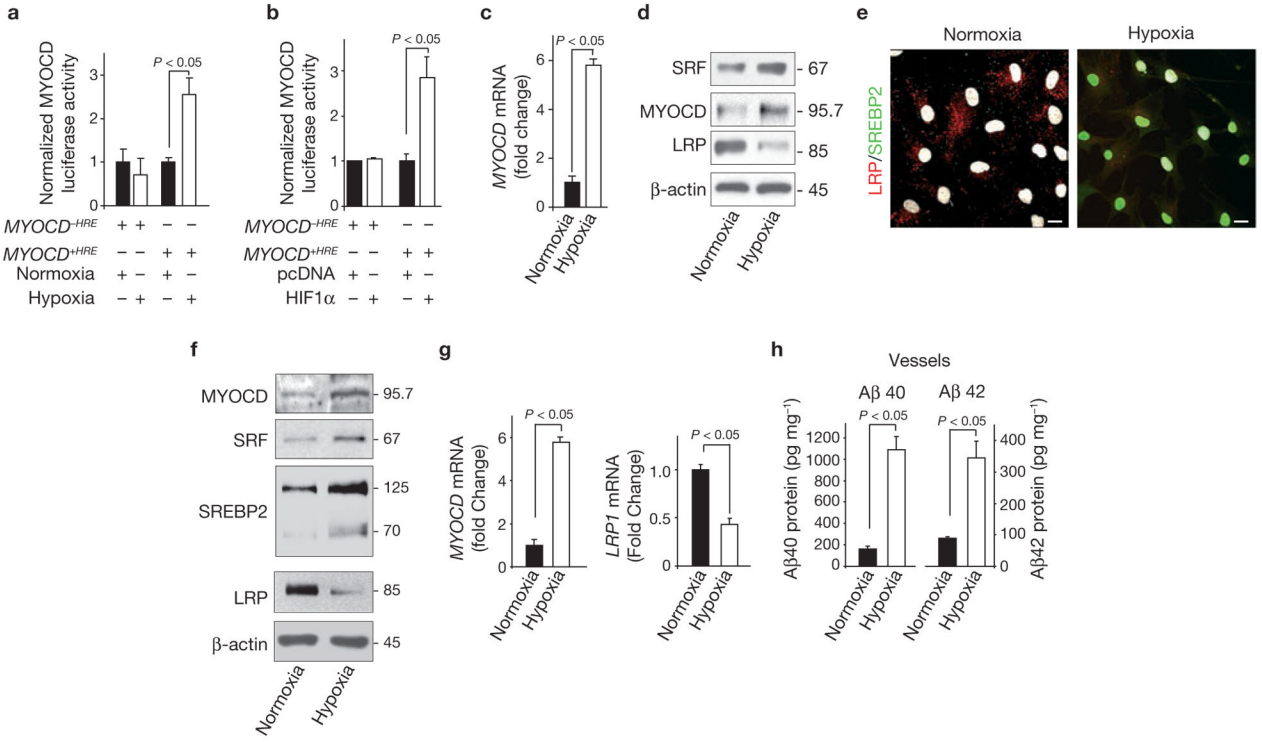

Figure 7.

Hypoxia increases MYOCD and SRF expression in human cerebral VSMC and pial vessels in *APPsw*$^{\pm}$ mice. (**a**) MYOCD luciferase activity in PAC1 VSMCs after transfection with a *luciferase* reporter, with or without the hypoxia response element (+HRE or −HRE) in the promoter region of human *MYOCD* gene. Cells were cultured for 48 h under normoxic or hypoxic (1% O_2) conditions. (**b**) MYOCD luciferase activity in PAC1 cells after transfection with a *luciferase* reporter with or without the HRE in the promoter region of human *MYOCD* gene and co-transfected with pcDNA vector or HIF-1α overexpression plasmid. Cells were cultured for 48 h under normoxic condition. (**c**) Real-time qPCR for *MYOCD* mRNA in control human cerebral VSMCs cultured for 48 h under normoxic or hypoxic (1% O_2) conditions. (**d**) MYOCD, SRF and LRP levels in control cerebral VSMCs within 48 h of normoxia or hypoxia. (**e**) Nuclear translocation of SREBP2 (green) and downregulation of LRP (red) in hypoxic human VSMCs within 48 h of hypoxia. Nuclear DAPI staining in white. Scale bars, 20 μm. (**f**) MYOCD, SRF, SREBP2 and LRP levels in isolated pial vessels from 5–6 month old *APPsw*$^{\pm}$ mice subjected to hypoxia (10–8% oxygen) or normoxia (21% oxygen) for 2 weeks. (**g**) Real-time qPCR for *MYOCD* and *LRP* mRNAs in pial vessels isolated from *APPsw*$^{\pm}$ mice treated as in **f**. (**h**) Aβ40 and Aβ42 levels in isolated pial vessels from *APPsw*$^{\pm}$ mice subjected to hypoxia or normoxia, as in **f**. In, Data represent mean ± s.e.m. of 3 independent cultures per group (**a–d**) or mean ± s.e.m. of 5 animals per group (**f–h**).

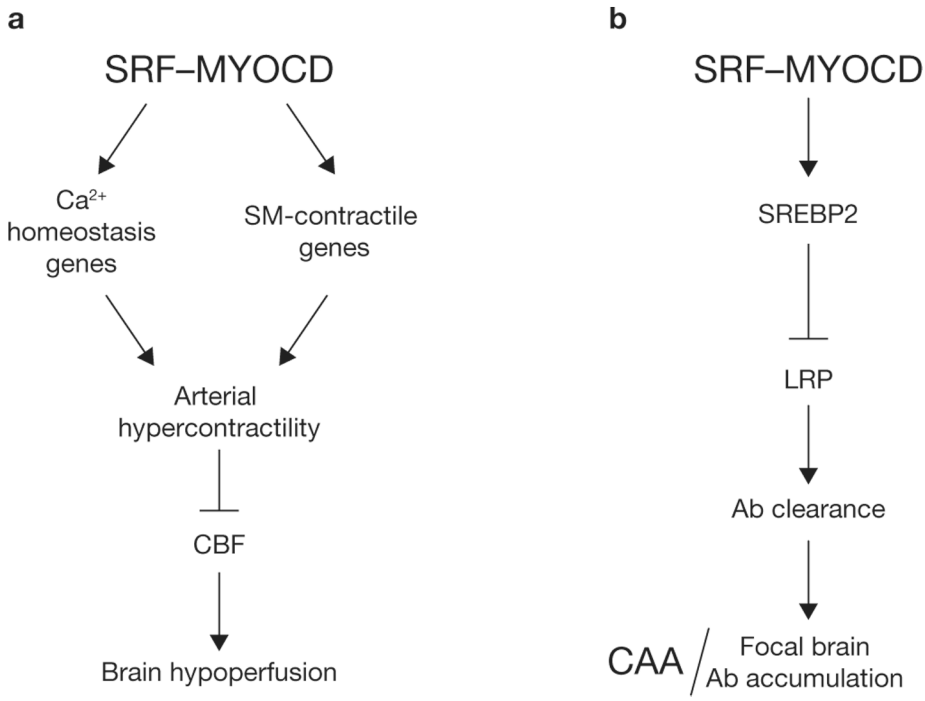

Figure 8.

SRF and MYOCD control blood flow and cerebral amyloid angiopathy (CAA). (**a**) Effects on cerebral blood flow (CBF). SRF and MYOCD overexpression in cerebral VSMC in AD stabilizes a VSMC hypercontractile phenotype through directed expression of the SRF-dependent genes which regulate Ca^{2+} homeostasis, for example, myosin light-chain kinase (*MYLK*), calsequestrin 1 (*CASQ1*), sarcoplasmic/endoplasmic reticulum calcium ATPase 2 (*ATP2A2*), and of SRF-MYOCD-regulated smooth muscle (SM) contractile genes, for example, SM myosin heavy chain (*MHC*), SM *α-actin*, *SM22α* and SM *calponin*, resulting in arterial hypercontractility and reductions in cerebral blood flow (CBF)[22]. (**b**) Pathological effects on CAA. SRF and MYOCD promote an Aβ non-clearing VSMC phenotype through directed expression of SREBP2, which acts as a transcriptional suppressor of LRP, a major clearance receptor for Aβ. This pathway leads to the development of CAA and limits local clearance of Aβ from brain tissue resulting in focal Aβ brain accumulations.